


REVIEW

Open Access



# Mitochondrial bioenergetic is impaired in Monocarboxylate transporter 1 deficiency: a new clinical case and review of the literature

Sinziana Stanescu<sup>1\*†</sup> , Irene Bravo-Alonso<sup>2†</sup>, Amaya Belanger-Quintana<sup>1</sup>, Belen Pérez<sup>2</sup>, Montserrat Medina-Díaz<sup>3</sup>, Pedro Ruiz-Sala<sup>4</sup>, Nathaly Paola Flores<sup>5</sup>, Raquel Buenache<sup>6</sup>, Francisco Arrieta<sup>7</sup> and Pilar Rodríguez-Pombo<sup>2</sup>

## Abstract

**Background:** Monocarboxylate transporter 1 (MCT1) deficiency has recently been described as a rare cause of recurrent ketosis, the result of impaired ketone utilization in extrahepatic tissues. To date, only six patients with this condition have been identified, and clinical and biochemical details remain incomplete.

**Results:** The present work reports a patient suffering from severe, recurrent episodes of metabolic acidosis and psychomotor delay, showing a pathogenic loss-of-function variation c.747\_750del in homozygosity in *SLC16A1* (which codes for MCT1). Persistent ketotic and lactic acidosis was accompanied by an abnormal excretion of organic acids related to redox balance disturbances. Together with an altered bioenergetic profile detected in patient-derived fibroblasts, this suggests possible mitochondrial dysfunction. Brain MRI revealed extensive, diffuse bilateral, symmetric signal alterations for the subcortical white matter and basal ganglia, together with corpus callosum agenesis.

**Conclusions:** These findings suggest that the clinical spectrum of MCT1 deficiency not only involves recurrent attacks of ketoacidosis, but may also cause lactic acidosis and neuromotor delay with a distinctive neuroimaging pattern including agenesis of corpus callosum and other brain signal alterations.

**Keywords:** Monocarboxylate transporter 1, Recurrent acidosis, Mitochondrial dysfunction, Psychomotor delay, White matter alterations, Corpus callosum agenesis

## Background

The monocarboxylate transporter (MCT) protein family is a diverse group of transmembrane proteins encoded by the *SLC16* gene family. These genes are distributed across all mammalian species and are involved in many metabolic pathways, including those used by the brain, skeletal

muscle, heart and tumor cells [1]. Of the 14 members of the *SLC16* family, MCT1 and MCT4 have been shown to undertake proton-coupled symport of important monocarboxylate metabolites, such as pyruvate, L-lactate and ketone bodies (acetoacetate and 3-hydroxy butyrate) [1–3].

MCT1, which is encoded by *SLC16A1*, is responsible for the import of monocarboxylates across the plasma membrane. It is expressed in nearly all human tissues, the most notable exception being the pancreatic  $\beta$ -cells. Genetic variations in *SLC16A1* have been associated with different human pathological conditions. Dominant gain-of-function mutations in the promoter region of

<sup>†</sup>Sinziana Stanescu and Irene Bravo-Alonso have contributed equally to this work

\*Correspondence: [sinziana.stanescu@salud.madrid.org](mailto:sinziana.stanescu@salud.madrid.org)

<sup>1</sup> Unidad de Enfermedades Metabólicas, Hospital Universitario Ramón y Cajal, IRYCIS, Crta de Colmenar Viejo, km 9,100, 28034 Madrid, Spain  
Full list of author information is available at the end of the article



*SLC16A1* provoking the abnormal expression of MCT1 in pancreatic  $\beta$ -cells have been identified in patients suffering from exercise-induced hyperinsulinemic hypoglycemia (MIM#610021), a clinical condition associated with dysregulated insulin secretion in states of low plasma glucose during anaerobic exercise [4].

Deficient MCT1 activity due to inactivating nucleotide changes in *SLC16A1* has been recorded in patients suffering from a ketone metabolism disorder caused by deficient ketone delivery to the extrahepatic tissues (MIM#616095). The first clinical description was made in 2014 in patients with severe recurrent episodes of ketosis, decreased consciousness and dehydration triggered by concurrent infections or fasting [5]. Since then, other authors have reported problems in biallelic homozygous patients, who, on top of recurrent ketoacidosis, also suffer from epilepsy and developmental delay, and who show neuroimaging anomalies of the subcortical white matter and basal ganglia, and/or agenesis of the corpus callosum [6, 7]. Interestingly, monoallelic carriers of variants in *SLC16A1* can also result in clinical symptoms such as cyclic vomiting and ketoacidosis [5, 8, 9]. In summary, MCT1 deficiency has been described in both monoallelic carriers with a potentially milder phenotype, and biallelic patients suffering a severe course of the disease. However, a combination of pathogenic variants in heterozygosity with other genetic and/or environmental factors has been suggested to contribute towards patients' clinical and biochemical phenotypes [8].

The present work reports the clinical and biochemical findings for a new patient with a homozygous mutation in *SLC16A1*. To understand the underlying pathophysiology involved, bioenergetic analyses were performed in patient-derived fibroblasts. The results clearly suggest a mitochondrial dysfunction not previously described.

## Materials and methods

Written informed consent to be included in this study was provided by the patient's parents. The study protocol adhered to the Declaration of Helsinki, and the protocol was approved by the Ethics Committee of *Universidad Autónoma de Madrid* (CEI-105-2052).

**Targeted analysis of metabolites** Organic acids in liquid urine samples were determined as trimethylsilyl derivatives by GC-MS after urease treatment and ethyl acetate liquid-liquid extraction without oximation [10].

## Genetic analysis

Genomic DNA was extracted from peripheral blood using the MagnaPure system (Roche Applied Science, Indianapolis, IN, USA) and subjected to massive parallel sequencing using the Nextera DNA Exome Kit (Illumina, San Diego, CA, USA) for whole exome sequencing

(WES). Variant calling was undertaken using DNAnexus (Mountain View, CA, USA) and an in-house bioinformatic pipeline. Overall mean exon coverage was  $78\times$ , with a  $\geq 20\times$  base coverage of 84%.

Variants were initially filtered based on their predicted pathogenicity and minor allele frequency ( $<0.005$ ). All genes with variants that survived this filtering were then screened using virtual panels based on phenotypic importance according to human phenotype ontology terms (HPO) [11] or the MitoCarta database [12].

Filtering also included the presence of gene variants previously annotated in the Human Gene Mutation Database (HGMD® Professional 2021.2) [13]. The potential pathogenicity of the selected variants was assessed using the VarSome web platform [14] which takes into account data from the dbSNP, ClinVar, gnomAD, RefSeq, Ensembl, dbNSFP, GERP, Kaviar, CIViC databases, and runs the DANN, dbNSFP, FATHMM, MetaLR, MetaSVM, Mutation Assessor, PROVEAN, GERP, LRT and MutationTaster-prediction programs.

## Cell culture

Healthy and patient-derived dermal fibroblasts obtained from a skin biopsy (taken with informed consent) were grown in minimal essential medium (MEM) supplemented with 1% glutamine, 10% foetal bovine serum (FBS), and antibiotics, following standard conditions. As healthy control-derived fibroblasts we used the cell lines CC2509 (Lonza, Basle, Switzerland) and GM8680 (Coriell Institute for Medical Research, Camden, NJ, USA). Most of experiments were accomplished when fibroblasts were at 80% confluence.

## Mitochondrial function

The cellular oxygen consumption rate (OCR) was measured in an XF24 Extracellular Flux Analyzer (Seahorse Bioscience, Izasa Scientific) according to [15], except that cells were raised in the same MEM as above but with galactose (1 g/L) instead of glucose during 24 h. After taking an OCR baseline measurement, oligomycin, carbonyl cyanide-4-(trifluoromethoxy) phenylhydrazone (FCCP), rotenone and antimycin A solutions were sequentially added to each well to reach final working concentrations 6  $\mu$ M, 20  $\mu$ M, 1  $\mu$ M and 1  $\mu$ M respectively. Each condition was measured three times every 7 min as indicated by the commercial kit. Basal respiration was measured without substrates. Oxygen consumption coupled to ATP production (ATP-linked) was calculated as the difference between basal respiration and the proton leak state determined after the addition of oligomycin. Maximum respiration was measured by stepwise 20  $\mu$ M titrations of FCCP and inhibition by rotenone and antimycin. Spare capacity was calculated as the difference between

maximum and basal respiration. Data are expressed as the OCR in picomoles per minute for 60,000 cells.

### Morphometric analysis of mitochondria

Morphometric analyses of mitochondria were made using a Jeol JEM-1010 (Jeol Ltd, Tokyo, Japan) electron microscope operating at 80 kVas, as described elsewhere [16]. Images were recorded with a 4 k CMOS F416 camera (TVIPS, Gauting, Germany). The aspect ratio was defined as the major axis/minor axis [17] and was measured in at least 50 randomly selected mitochondria. A minimum aspect ratio of 1 corresponds to a perfect circle.

### Mitochondrial isolation and Western blotting

Mitochondria were isolated using the hypotonic swelling procedure [18]. These mitochondria were then denatured in Laemmli buffer for 5 min at 50 °C, and extracts subjected to SDS-PAGE separation and Western blotting [15]. For native PAGE analysis, protein samples were prepared following the indications provided with the NativePAGE™ Novex® Bis-Tris Gel System (Invitrogen, Carlsbad, CA, USA). Fifteen micrograms of mitochondrial sample were resuspended in a medium with 2% digitonine, and then loaded onto 3–12% NativePAGE™ Novex gel. The primary polyclonal antibodies used were: anti-total OxPhos (NDUFB8-CL, SDHB-CII, UQCRC2-CIII, MTCOI-CIV and ATP5A-CIV) (ab110413; Abcam, Cambridge, UK), anti-NDUFA9 (ab14705, Abcam), anti-MTCOI (ab14705, Abcam) and anti-ATP5A (ab14748, Abcam). Anti-citrate synthase (C5498, Sigma Aldrich) and anti-SDHA (ab14715, Abcam) were used as loading controls. Films were scanned and densitometered using the BioRad GS-900 scanner and Image Lab 5.2 software.

### Statistical analysis

Values are expressed as means ± SEM of 'n' independently performed experiments in cultured cells. Differences between means were examined using the Student t test. Significance was set at  $p < 0.05$ . All calculations were performed using GraphPad Prism 6 (GraphPad Software, La Jolla, CA, USA).

## Results

### Case report

The present patient, a female infant, is the second child of non-consanguineous Moroccan parents. There was no relevant family history; her oldest brother was diagnosed at the age of 8 years old of type I diabetes mellitus. Corpus callosum agenesis (HP:0001274) was detected during prenatal monitoring and later confirmed by clinical assessment. Her birth and perinatal period were normal. At the age of 4 months she had an episode of

severe acidosis (pH 6.7) (HP:0001942) during a respiratory infection. Plasma 3-hydroxy butyrate and lactate levels were increased at 2.3 mmol/L (HP:0033419) and 7.0 mmol/L (HP:0003128) respectively; ammonia, glucose, and liver function remained normal. She was diagnosed with sepsis, treated with antibiotics and fluid replacement, and made a full recovery. No further metabolic studies were performed. At the age of 15 months she suffered two more episodes of severe acidosis (pH 7.0 on both occasions) associated with dehydration and reduced consciousness (HP:0007185) following vomiting (HP:0002013) and fasting. She was admitted to a regional hospital and her condition improved with continuous infusion of dextrose. Her plasma lactate was mildly elevated (2.6 mmol/L) and her glucose slightly low (2.5 mmol/l) (HP:0001943), but no ketone body analysis was performed during the initial check-up.

After these episodes she was transferred to our metabolic unit for further investigation. In her basal state, she persistently maintained mildly elevated lactate plasma levels (2.3–2.5 mmol/L); urine gas chromatography showed increased excretion of ketone bodies (HP:0410175), lactate, 2-hydroxy butyrate and 3-hydroxy isovalerate, all compatible with an underlying mitochondrial disorder (see Table 1). Slight elevation of plasma alanine (Ala) was detected in one determination, but it was not sustained (see Table 1). Lactate and amino acids levels in cerebrospinal fluid were normal in basal state [lactate: 1.67 mM, Ala: 30 μmol/L (NV: 30 ± 11)].

A fasting test was performed and after 18 h the patient showed hypoglycemia (2.2 mmol/L) with ketosis (3-hydroxy butyrate: 5.2 mmol/L) and significant metabolic acidosis with a pH of 7.28, a plasma bicarbonate concentration of 7.5 mmol/L, and base excess of −17.5 mmol/L. She was treated with continuous infusion of dextrose and bicarbonate supplements. Metabolic studies made during her fasting revealed the massive excretion of 3-hydroxy butyrate, acetoacetate, lactate, 2-hydroxy butyrate and 3-hydroxyisovalerate (see Table 1).

A brain MRI performed at the age of 23 months revealed diffuse, bilateral, symmetric signal alterations for the subcortical supratentorial white matter, with an anteroposterior gradient, especially significant in the frontal and insular areas. These alterations consisted of hyperintensity in the T2-weighted sequence (HP:003090) (Fig. 1A, B) affecting the U fibers, a hypersignal in the diffusion-weighted sequence (Fig. 1C, D), and low apparent diffusion coefficient (ADC) values (Fig. 1E, F). This same pattern of signal alteration was seen in the Probst bands (Fig. 1, red arrow), in the anterosuperior and medial regions of the thalamus (Fig. 1, blue arrow), and in both putamens, especially in the globus pallidus (Fig. 1,

**Table 1** Metabolic study at different times in the patient’s life and after 18 h of fasting

| Age  | 7 Months (no acidosis) | 10 Months (no acidosis) | 15 Months (no acidosis) | 15 Months, 18 h of fasting               |
|--|------------------------|-------------------------|-------------------------|--|
| <i>Urine organic acids (mmol/mol creatinine)</i> |                        |                         |                         |  |
| 3-Hydroxy butyrate (NV: 2–17)                    | 158                    | 1114                    | 284                     | 15,471                                   |
| Acetoacetate (NV: 0–7)                           | 117                    | 792                     | 20                      | 9342                                     |
| Lactate (NV: 5–113)                              | 9312                   | 359                     | 28                      | 23,846                                   |
| 2-Hydroxy butyrate(NV: 0–4)                      | 380                    | 273                     | 15                      | 11,944                                   |
| 3-Hydroxy isovalerate (NV: 1–40)                 | 56                     | 56                      | 19                      | 315                                      |
| <i>Plasma amino acids (μmol/L)</i>               |                        |                         |                         |  |
| Alanine (NV: 297 ± 96)                           | 435                    | 230                     | 329                     | 124                                      |
| Others   | Normal                 | Normal                  | Normal                  | Elevation of BCAA due to severe ketosis  |
| <i>Plasma acylcarnitines μmol/L</i>              |                        |                         |                         |  |
|  | Normal                 | Normal                  | Normal                  | Mild elevation of C12–C14 due to ketosis |

NV normal value, C12 dodecanoylcarnitine, C14 myristoylcarnitine, BCAA branched-chain amino acids

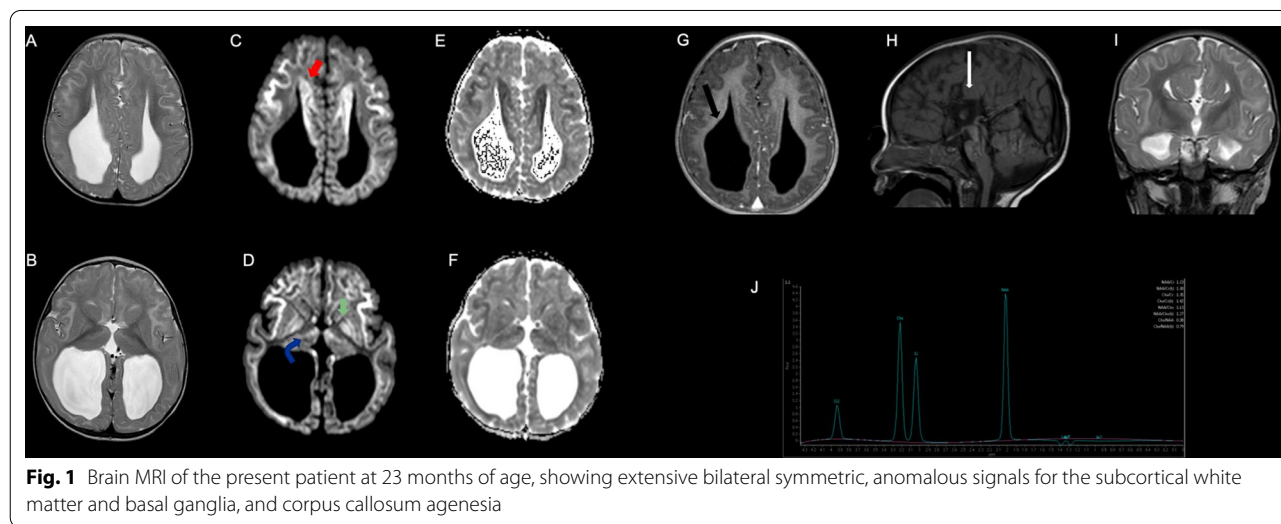


**Fig. 1** Brain MRI of the present patient at 23 months of age, showing extensive bilateral symmetric, anomalous signals for the subcortical white matter and basal ganglia, and corpus callosum agenesis

green arrow). No enhancement was observed in the T1-weighted sequence after intravenous contrast administration (Fig. 1G). She also showed complete agenesis of the corpus callosum (HP:0001274) (Fig. 1, white arrow) with colpocephaly (HP:0030048) (Fig. 1, black arrow) and marked loss of volume of the predominantly posterior white matter (Fig. 1G–I). Single voxel, long TE proton MRI spectroscopy showed no pathological peak for lactate (Fig. 1J).

Frequent feeding (maximum fasts of 6 h) and adequate energy intake were recommended during episodes of illness. She has had no further acute episodes of acidosis and/or ketosis, and her current plasma lactate levels are normal. At the age of 6 years, clinical examination revealed moderate psychomotor delay (HP:0001263); she has an unsteady gait (HP:0002317) due to axial

hypotonia (HP:0008936) and her language skills are poor (HP:0002463).

Although a ketolytic defect was the main clinical suspicion, she was included in a genetic testing program designed for patients showing persistent lactic acidosis, and was classified as having a *probable mitochondrial disorder*. The mitochondrial disease score was based on the sum of her clinical and biochemical symptoms according to the Nijmegen system, modified by Morava et al. [19].

### Mitochondrial function

To assess the mitochondrial functionality, we accomplished a real-time oxygen consumption test, visualised the mitochondrial ultrastructure and evaluated the presence of OxPhos proteins, both individually or ensembled in respiratory complexes. To force a mitochondrial

synthesis of ATP, controls and patient fibroblasts were grown in galactose-media. The Seahorse data revealed a robust reduction in maximum respiration and spare capacity comparison to controls, indicating diminished cell capacity to respond to stress stimuli or higher metabolic demands (Fig. 2A). In concordance with these results, we observed an altered mitochondria ultrastructure of patient-derived fibroblasts with disrupted cristae structure (Fig. 2B—white arrows) and significant increases in the number of elongated mitochondria (Fig. 2C), all compatible with an energetic challenge. Mitochondria from control cells showed a characteristic zebra-striped appearance.

Finally, Western blotting analysis of OxPhos proteins and respiratory complex in mitochondrial extracts revealed a notable reduction in the fully assembled CI (Fig. 2E) of the patient compared to control analyzed by Blue Native PAGE. No major changes were detected in either other complexed or individual OxPhos proteins visualized by SDS-PAGE (Fig. 2D).

#### Genetic analysis

In an early genetic analysis of the clinical exome, the change NM\_003051.4:c.747\_750del (p.Asn250Serfs\*5) was identified in homozygous fashion in *SLC16A1* [15]. This variant had been previously described in monoallelic carriers patients with ketoacidosis and massive ketonuria [5]. Sanger sequencing confirmed the presence of this change in heterozygous fashion in the patient's healthy progenitors and one sibling. According to the literature, the presence of c.747\_750del explains the persistent ketoacidosis, but not the mitochondrial dysfunction signature. Other possible changes in genes not included in the clinical exome panel were thus sought, performing WES of the patient's DNA. The inclusion of a third filtering step based on HPO terms, or including all genes from the MitoCarta database [20] in the narrowing down of genetic-variants discovered by WES, corroborated the presence of the above change but also identified NM\_018480.7: c.83T>C (p.Val28Ala) in homozygous fashion in *TMEM126B*, which encodes a

transmembrane component of the mitochondrial complex I. Biallelic changes in *TMEM126B* has been related to the mitochondrial complex I deficiency, nuclear type 29 (MIM#618250). However, this last change, classified as -likely benign- according to the VarSome web platform [14, 21] and as -tolerant- by the recently developed MetaDome web server [22, 23] was discarded as disease-causing based on the existence of two homozygotes for c.83T>C, who show no sign of disease (recorded on the gnomAD platform [24]). No changes in mitochondrial DNA were detected. A complete list of genes and variants identified via WES is provided in Additional file 1, which also compiled consideration for discarding other changes such as those identified in *PHKA2* or *SLC3A1*.

#### Literature review

Up to now, 14 patients, included two siblings, having a MCT1 deficiency have been reported. Six were with biallelic pathogenic variants all harboured in homozygous fashion and for the remaining, monoallelic nucleotide changes were reported (see Table 2). Mutational spectrum included two duplications, three deletions, three nonsense changes and one missense change [5–7]. Although several cases of symptomatic monoallelic carriers have been described, not all the carriers display symptoms [8, 9], even when the same mutation is involved, suggesting that possible triggers are also needed for the development of the recurrent ketoacidosis.

The age at diagnosis varied between 3–23 months for the homozygous patients. Clinically these patients present severe ketoacidosis episodes during glucose shortage events such as infections or fasting (see Table 2). During the metabolic crisis, they received treatment with dextrose infusion together with sodium bicarbonate to correct the acidosis [5–7]. Interestingly, although the ketoacidosis crisis may be present at 3 days of life [6], after the age of 7–8 years old there seems to be a complete resolution of the metabolic crisis, which might suggest adaptative mechanisms or environmental factors [5, 7, 8]. The present patient had the last documented ketoacidosis attack at the age of 15 months.

(See figure on next page.)

**Fig. 2** **A** Oxygen consumption rates of control (C) and patient-derived (Pt) fibroblasts measured in MEM with galactose (1 g/L) (GAL) instead of glucose, and upon the subsequent addition of (a) 6  $\mu$ M oligomycin (OL), (b) 20  $\mu$ M FCCP, (c) 1  $\mu$ M rotenone and 1  $\mu$ M antimycin (R/A). Oxygen consumption coupled to ATP production (ATP-linked), maximum respiration (Rmax) and spare capacity (Spare) were calculated for each situation. Results are expressed as fold-change over the control concentrations and are the mean  $\pm$  SD of 3–5 wells from three independent experiments represented by circles in the bar graph. Control values are the means of the two control cell lines (CC2509 and GM8680). **B** Electron microscopy images showing defects in mitochondrial ultrastructure and cristae organization (white arrows) in patient-derived fibroblasts grown in MEM with galactose. Mitochondrial length was determined in control (C) and patient-derived (Pt) fibroblasts. **C** Mitochondrial enlargement is expressed as the aspect ratio (major/minor mitochondrial axis ratio). Measurements were made for at least 50 mitochondria. Statistical analysis were performed using GraphPad Prims software. Student t test (\*\* $p$  < 0.01; \*\*\* $p$  < 0.001). **D** Western blot of Oxphos (SDS-PAGE-separated) from purified mitochondria. **E** Blue native gel, staining of complex I (NDUFA9), complex II (SDHA), complex IV (MTCOI) and complex V (ATP5A) in purified mitochondria CI: complex I; CII: complex II; CIII: complex III; CIV: complex IV; CV: complex V; CS: Citrate Synthase; SC: supercomplexes

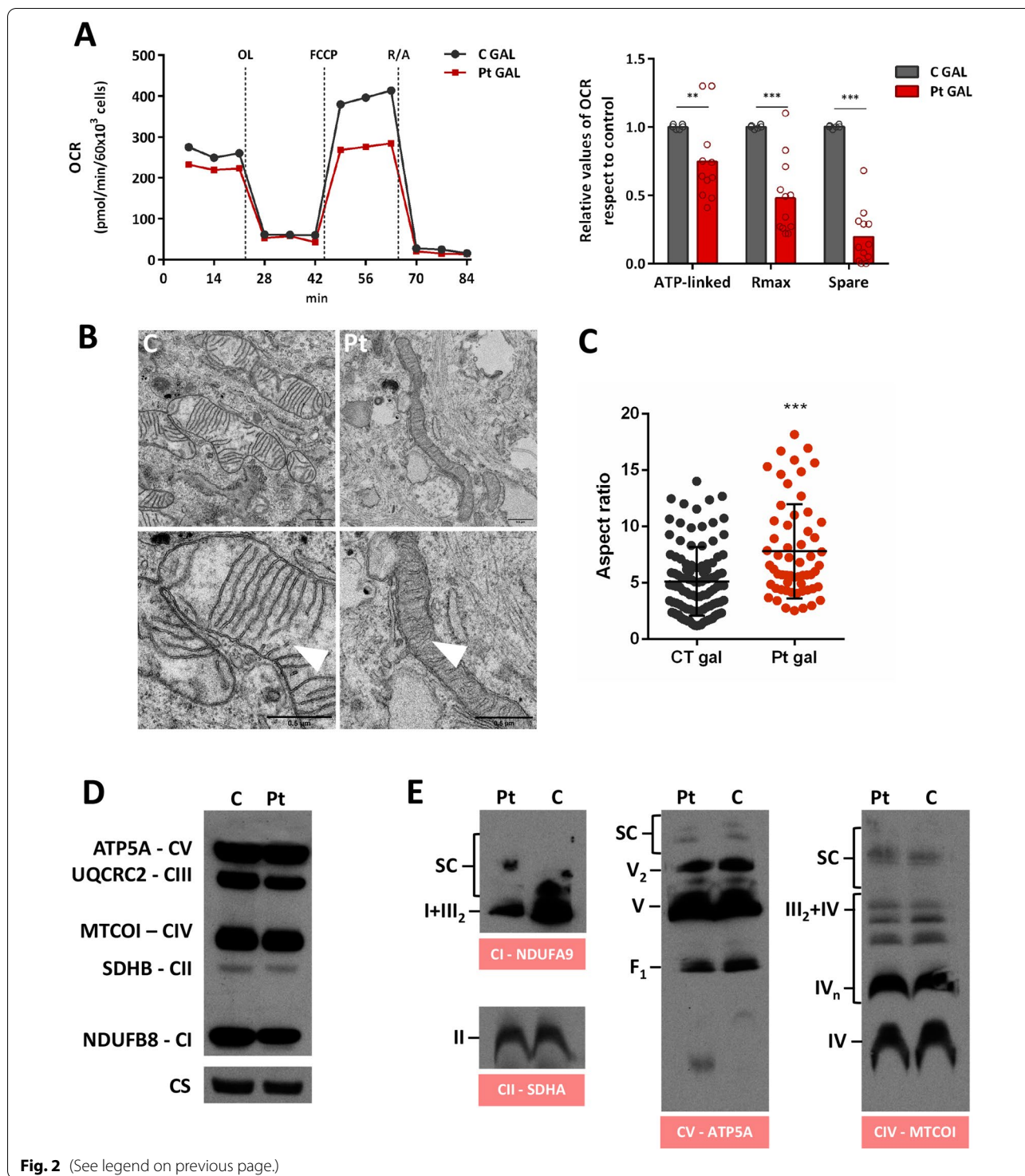


**Fig. 2** (See legend on previous page.)

Moreover, the homozygous patients have common central nervous clinical features like psychomotor delay, epilepsy or corpus callosum agenesis, with a distinctive neuroimaging pattern [5–7], differently from other

inborn errors of ketone utilization like succinyl CoA oxoacid transferase (SCOT) deficiency (MIM#245050) and mitochondrial acetoacetyl-CoA thiolase (ACAT1) deficiency (MIM#203750) [25].

**Table 2** Characteristics of the patients with MCT1 deficiency

|                           |                                   | van Hasselt, 2014               |                                 |                                 |  | Al-Khawaga 2019                     |                                     | Nicolas-Jilwan, 2020;2015          |  | Balasubramaniam, Le, 2020                                    |  |   |
|---------------------------|-----------------------------------|---------------------------------|---------------------------------|---------------------------------|--|-------------------------------------|-------------------------------------|------------------------------------|--|--|--|---|
| Ethnicity                 | Syrian                            | Irish                           | Turkish                         | British                         | British                                | Dutch                               | Dutch                               | nr                                 | nr   | nr   | Sephardic Jewish   |   |
| Consanguinity             | Yes                               | No                              | Yes                             | Yes                             | Yes                                    | Yes                                 | Yes                                 | Yes                                | Yes  | Yes  |  |   |
| Allele 1 (Variant/Effect) | <b>c.41dup (p. Asp15Argfs*34)</b> | <b>c.937C&gt;T (p. Arg313*)</b> | <b>c.982C&gt;T (p. Arg328*)</b> | <b>c.586C&gt;T (p. Arg196*)</b> | <b>c.747_750del (p. Asn250Serfs*5)</b> | <b>c.499del (p. Val167Phefs*13)</b> | <b>c.490dup (p. Leu164Profs*46)</b> | <b>c.938G&gt;A (p. Arg313Gln)†</b> | <b>c.218del (p. Gly73Valfs*8)</b>  | <b>c.1079del (p. Ala360Glyfs*19)</b>                         | <b>c.982C&gt;T (p. Arg328*)</b>  |   |
| Allele 2 (Variant/Effect) | <b>c.41dup (p. Asp15Argfs*34)</b> | <b>c.937C&gt;T (p. Arg313*)</b> | <b>c.982C&gt;T (p. Arg328*)</b> | –                               | –                                      | –                                   | –                                   | –                                  | <b>c.218del (p. Gly73Valfs*8)</b>  | <b>c.1079del (p. Ala360Glyfs*19)</b>                         | <b>c.41dup (p. Asp15Argfs*34)</b>  |   |
| Metabolic derangement     | Profound ketoacidosis             | Profound ketoacidosis           | Profound ketoacidosis           | Cyclic vomiting                 | Ketoacidosis                           | Ketoacidosis                        | Ketoacidosis                        | Cyclic vomiting                    | Recurrent attacks of hypoglycemia and metabolic acidosis; massive ketonuria, normal acid lactic  | Recurrent ketoacidosis, no hypoglycemia                      | Recurrent ketoacidosis, no hypoglycemia  | Recurrent ketoacidosis, no hypoglycemia |
| Metabolic screening       | –                                 | –                               | –                               | –                               | –                                      | –                                   | –                                   | –                                  | Normal serum ammonia, lactate, and pyruvate, amino acids, and acyl carnitine. Normal urine succinyl acetone, orotic, and organic acids | Normal plasma lactate, and ammonia                           | Normal serum ammonia and lactate. Massive ketonuria, increased urine 2-methyl-3-hydroxybutyrate, 2-methylacetate and tiglylglycine | –                                       |
| Additional notes          |                                   |                                 |                                 |                                 |  |                                     |                                     |                                    |  | Sibling of the previous patient (no genetic study performed) |  |   |

**Table 2** (continued)

| van Hasselt, 2014        |  | Al-Khawaga 2019                  |                              | Nicolas-Jilwan, 2020; 2 siblings |         | Balasubramaniam, 2015 |                      | Le, 2020  |  |                                   |                  |
|--------------------------|--|----------------------------------|------------------------------|----------------------------------|---------|-----------------------|----------------------|---|--|-----------------------------------|------------------|
| Ethnicity                | Syrian   | Irish                            | Turkish                      | British                          | British | Dutch                 | Dutch                | nr  | nr   | British                           | Sephardic Jewish |
| Brain MRI                | –  | –                                | –                            | –                                | –       | –                     | –                    | Heterotopia, white matter diffuse alterations. Normal spectroscopy (no lactate elevation) | White matter diffuse alteration, including basal ganglia, corpus callosum agenesis | –                                 | Normal           |
| Epilepsy                 | –  | Yes                              | –                            | –                                | –       | –                     | –                    | Yes   | Yes  | Generalized tonic-clonic seizures | Absent seizures  |
| Psychomotor delay        | Moderate intellectual disability   | Moderate intellectual disability | Mild intellectual disability | –                                | –       | –                     | –                    | Normal at the age of 18 months  | Motor and speech delay   | Developmental delay               | –                |
| Congenital malformations | Atrial septal defect, hypoplastic left pulmonary artery, and main bronchus | –                                | Cleft palate                 | –                                | –       | –                     | –                    | –   | –  | Left kidney agenesis              | –                |
| Others                   | Microcephaly   | –                                | –                            | Migraine                         | –       | Short stature         | Exercise intolerance | –   | –  | Failure to thrive                 | Microcephaly     |
|                          |  |                                  |                              |                                  |         |                       |                      |   |  | Fatty liver                       |                  |

The bold corresponds to biallelic pathogenic variants

Variant nomenclature follows the recommendations of Human Genome Variation Society (HGVS) (<https://varnomen.hgvs.org/>)



## Discussion

The details of MCT1 deficiency remain to be understood. To the best of our knowledge there are only six patients with biallelic pathogenic variants causing MCT1 deficiency reported up to now in the literature, see Table 2 [5–7]. These patients all suffered recurrent episodes of severe ketoacidosis during catabolic events such as fasting or infection, especially in their first years of life. Moreover, patients with a monoallelic change in *SLC16A1* also experience recurrent episodes of acidosis, see Table 2 [5, 8, 9], suggesting that monoallelic carriers may be more prevalent than would seem apparent. The present patient suffered several severe episodes of metabolic acidosis due to ketosis, but also had lactate accumulation. Her monoallelic carrier family members experienced no cyclic vomiting or recurrent ketosis, but none underwent any biochemical study. Notwithstanding that the absence of any remarkable symptomatology has previously been reported in family members of other patients with monoallelic pathogenic changes for *SLC16A1* [8], the health status of mutation carriers should be monitored for possible late manifestation of the disease.

Apart from the ketoacidosis attacks, the biallelic variants for MCT1 deficiency patients described so far also present other common features such as important central nervous system involvement including neuroimaging abnormalities, psychomotor delay, epilepsy and agenesis of corpus callosum [5–7]. That might reveal the consequences that MCT1 deficiency might have on brain energy homeostasis.

MCT1 is responsible for the H<sup>+</sup>-coupled transport of short chain monocarboxylates, primarily L-lactate, pyruvate or ketone bodies that enter the mitochondria as respiratory fuel [26]. Indeed, MCT1 has been described as a major player in whole-body energy homeostasis and the distribution of redox potential between organs [27]. To date, however, lactic acidosis has not been detected in patients with MCT1 deficiency. Recent studies in the Schwann cells of MCT1 knockout mice, have, nonetheless, detected reductions in spare respiratory capacity similar to those seen in the present patient, leading to impaired mitochondrial function [28].

The central nervous system is highly dependent on a continuous energy supply. The human brain accounts for some 20% of the body's total expenditure at rest [29, 30], while the developing brain consumes 40% [31]. Glucose is the main fuel employed, and glucose transporters ensure its efficient uptake by neural cells. During glucose shortage events, however, such as fasting or catabolic episodes, the brain can metabolize other organic substrates, especially lactic acid and ketone bodies [32]. Monocarboxylate transporters play a crucial role in the use of

these substrates [33]. In recent years, a growing body of evidence has revealed lactate to be an energy substrate for the brain as well, sustaining its neuronal activity during glucose deprivation [34–37]. The hyperlactacidemia observed during hypoglycemia episodes in glycogen storage disease type I might be another example [25]. It has also been suggested that monocarboxylates represent substantial energy substrates, especially for the developing brain [38, 39]. For example, lactate is elevated in newborns' blood immediately after delivery, providing an important brain energy substrate for the first few hours after birth [40]. In neonatal mice, brain lactate is successfully utilized in the hippocampus as an energy substrate, and maintains synaptic function [41]. Ketone bodies are also an important source of energy for the brain under certain conditions, including fasting, ketogenic diets, and in breastfed newborn babies [42–44].

Interestingly, it has been recently shown that monocarboxylates might also be involved in more complex metabolic pathways such as myelin synthesis. In rat cerebellum and corpus callosum, white matter oligodendrocytes take up lactate via MCT1 to ensure neuron survival and myelination in low-glucose conditions [45, 46]. Moreover, in animal studies oligodendrocytes progenitor cells involved in myelination utilize lactate for cell cycling and differentiation in metabolic pathways in which MCT1 is a central figure. This has important implications in high myelin brain regions such as the corpus callosum [47, 48].

From this point of view, the MCT1 deficiency induces impaired monocarboxylate transport and might be involved in important energetic perturbations in nervous system energy metabolism that become more evident during glucose shortage events and could affect important processes such as myelination in the developing brain. That may explain the presence of MRI findings in high myelin brain regions like basal ganglia or corpus callosum and clinical features such as psychomotor delay or epilepsy. This hypothesis is supported by the present bioenergetic analysis performed with the patient's fibroblasts. Here, the maximal mitochondrial oxygen consumption capacity following the addition of FCCP, which mimics a physiologic energy demand, was significantly decreased, confirming an impaired capacity for adapting to stress. The remodelling seen in mitochondrial size and the appearance of the cristae might be the response to the energetic challenge posed, as changes in cellular metabolic demands or homeostatic insults are known to correlate with changes in the mitochondrial ultrastructure [49]. It remains to be clarified whether other genetic variations influence mitochondrial fitness to adapt.

In summary, while MCT1 deficiency is associated with recurrent episodes of ketoacidosis, it may also involve episodes of lactic acidosis, neuromotor delay and neuroimaging anomalies of the subcortical white matter and basal ganglia or agenesis of the corpus callosum. The multiple pathways that monocarboxylates might follow in the neurons and glia, such as the production of ATP or myelin synthesis, might explain the complex features associated with biallelic MCT1 deficiency. MCT1 phenotype is probably the result of a plethora of causes including a dosage effect of the *SLC16A1* variants, but also the result of other contributors such as combinations of cis or trans-acting changes that should be relevant for the global response to an energetic shortage.

## Supplementary Information

The online version contains supplementary material available at <https://doi.org/10.1186/s13023-022-02389-4>.

**Additional file 1:** A complete list of genes and variants identified via WES.

### Author contributions

SS and IBA had a significant contribution to the conception and design of the study. IBA and PRP performed the bioenergetic analyses in patient-derived fibroblasts. BP and IBA carried out the genetic analysis and interpretation of the data. MMD performed the neuroimaging interpretation. NPF and RB provided clinical details and psychomotor development evaluation of the patients. ABQ and FA contributed to the acquisition and interpretation of the data. PRS carried out the organic acid determination in liquid urine. All authors read and approved the final manuscript.

### Funding

This work was funded by grant PI19/01155, B2017/BMD-3721 and the European Regional Development Fund. Open Access is supported by Fundación Ramón Areces (Grant No. C1VP17A2827).

### Availability of data and materials

All data generated or analyzed during this study are included in this published article and its supplementary information files.

## Declarations

### Ethics approval and consent to participate

The study protocol adhered to the Declaration of Helsinki, and the protocol was approved by the Ethics Committee of *Universidad Autónoma de Madrid* (CEI-105-2052). No animals were used in this study. Written informed consent to be included in this study was provided by the patient's parents.

### Consent for publication

Written informed consent for publication was provided by the patient's parents.

### Competing interests

SS has received travel and speaker fees from Nutricia, Mead Johnson, Genzyme, Recordatti Rare Diseases, Vitaflor-Nestlé, BioMarin. IBA declares that she has no conflict of interest. ABQ has received travel and speaker fees from Nutricia, Mead Johnson, Genzyme, Recordatti Rare Diseases, Vitaflor-Nestlé, Takeda, BioMarin; advisory fees from BioMarin and Merk Serono. FA has received travel and speaker fees from Nutricia, Mead Johnson, Recordatti Rare Diseases, Vitaflor-Nestlé, BioMarin. MMD declares that she has no conflict of interest. PRS declares that she has no conflict of interest. BP declares that she has no conflict of interest. NPF declares that she has no conflict of interest. RB declares that she has no conflict of interest. PRP declares that she has no conflict of interest.

## Author details

<sup>1</sup>Unidad de Enfermedades Metabólicas, Hospital Universitario Ramón y Cajal, IRYCIS, Crta de Colmenar Viejo, km 9,100, 28034 Madrid, Spain. <sup>2</sup>Centro de Diagnóstico de Enfermedades Moleculares, Centro de Biología Molecular Severo Ochoa, UAM-CSIC, CIBERER, IdiPAZ, C/Francisco Tomás y Valiente, 7, 28049 Madrid, Spain. <sup>3</sup>Department of Neuroradiology, Hospital Universitario Ramón y Cajal, IRYCIS, Crta de Colmenar Viejo, km 9,100, 28034 Madrid, Spain. <sup>4</sup>Centro de Diagnóstico de Enfermedades Moleculares, Centro de Biología Molecular, Universidad Autónoma de Madrid, CIBERER, IdiPAZ, C/Francisco Tomás y Valiente, 7, 28049 Madrid, Spain. <sup>5</sup>Paediatric Department, Hospital General La Mancha Centro, Av. Constitución, 3, 13600 Alcázar de San Juan, Ciudad Real, Spain. <sup>6</sup>Neuropediatric Department, Hospital Universitario Ramón y Cajal, IRYCIS, Crta de Colmenar Viejo, km 9,100, 28034 Madrid, Spain. <sup>7</sup>Unidad de Enfermedades Metabólicas, Hospital Universitario Ramón y Cajal, IRYCIS, CIBER-OBN, Crta de Colmenar Viejo, km 9,100, 28034 Madrid, Spain.

Received: 3 March 2022 Accepted: 6 June 2022

Published online: 21 June 2022

## References

- Halestrap AP. The SLC16 gene family—structure, role and regulation in health and disease. *Mol Aspects Med.* 2013;34:337–49.
- Halestrap AP, Meredith D. The SLC16 gene family—from monocarboxylate transporters (MCTs) to aromatic amino acid transporters and beyond. *Pflugers Arch.* 2004;447:619–28.
- Hediger MA, Clémenton B, Burrier RE, Bruford EA. The ABCs of membrane transporters in health and disease (SLC series): introduction. *Mol Aspects Med.* 2013;34:95–107.
- Palladino AA, Bennett MJ, Stanley CA. Hyperinsulinism in infancy and childhood: when an insulin level is not always enough. *Clin Chem.* 2008;54(2):256–63.
- van Hasselt PM, Ferdinandusse S, Monroe GR, Ruiten JP, Turkenburg M, Geerlings MJ, et al. Monocarboxylate transporter 1 deficiency and ketone utilization. *N Engl J Med.* 2014;371:1900–7.
- Al-Khawaga S, AlRayahi J, Khan F, Saraswathi S, Hasnain R, Haris B, et al. A SLC16A1 mutation in an infant with ketoacidosis and neuroimaging assessment: expanding the clinical spectrum of MCT1 deficiency. *Front Pediatr.* 2019;7:299. <https://doi.org/10.3389/fped.2019.00299>.
- Nicolas-Jilwan M, Medlej R, Sulaiman RA, AlSayed M. The neuroimaging findings of monocarboxylate transporter 1 deficiency. *Neuroradiology.* 2020;62:891–4.
- Balasubramaniam S, Lewis B, Greed L, Meili D, Flier A, Yamamoto R, et al. Heterozygous monocarboxylate transporter 1 (MCT1, SLC16A1) deficiency as a cause of recurrent ketoacidosis. *JIMD Rep.* 2016;29:33–8.
- Le A, Yeganeh M, Buhás D, Trempe MJ, Myers KA. Monocarboxylate transporter-1 deficiency results in severe metabolic acidosis with ketogenic diet in early onset absence epilepsy: case report. *Seizure.* 2020;74:31–2.
- Rodríguez JM, Ruíz-Sala P, Ugarte M, Peñalva MA. Fungal metabolic model for 3-methylcrotonyl-CoA carboxylase deficiency. *J Biol Chem.* 2004;279:4578–87.
- Köhler S, Gargano M, Matentzoglou N, Carmody LC, Lewis-Smith D, Vasilevsky NA, et al. The human phenotype ontology in 2021. *Nucleic Acids Res.* 2021;49:D1207–17.
- <https://www.broadinstitute.org/files/shared/metabolism/mitocarta/human.mitocarta2.0.html>.
- <https://portal.biobase-international.com/hgmd/pro/start.php>.
- <https://varsome.com>.
- Bravo-Alonso I, Navarrete R, Vega AI, Ruíz-Sala P, García Silva MT, Martín-Hernández E, et al. Genes and variants underlying human congenital lactic acidosis—from genetics to personalized treatment. *J Clin Med.* 2019;8:1811.
- Oyarzabal A, Bravo-Alonso I, Sánchez-Aragó M, Rejas MT, Merinero B, García-Cazorla A, et al. Mitochondrial response to the BCKDK-deficiency: some clues to understand the positive dietary response in this form of autism. *Biochim Biophys Acta.* 2016;1862:592–600.
- De Vos KJ, Allan VJ, Grierson AJ, Sheetz MP. Mitochondrial function and actin regulate dynamin-related protein 1-dependent mitochondrial fission. *Curr Biol.* 2005;15:678–83.

18. Mohanraj K, Wasilewski M, Benincá C, Cysewski D, Poznanski J, Sakowska P, et al. Inhibition of proteasome rescues a pathogenic variant of respiratory chain assembly factor COA7. *EMBO Mol Med*. 2019;11:e9561.
19. Morava E, van den Heuvel L, Hol F, de Vries MC, Hogeveen M, Rodenburg RJ, et al. Mitochondrial disease criteria: diagnostic applications in children. *Neurology*. 2006;67:1823–6.
20. Calvo SE, Clauser KR, Mootha VK. MitoCarta2.0: an updated inventory of mammalian mitochondrial proteins. *Nucleic Acids Res*. 2016;44:D1251–7.
21. Kopanos C, Tsiolkas V, Kouris A, Chapple CE, Albarca Aguilera M, Meyer R, et al. VarSome: the human genomic variant search engine. *Bioinformatics*. 2019;35:1978–80.
22. Wiel L, Baakman C, Gilissen D, Veltman JA, Vriend G, Gilissen C. MetaDome: pathogenicity analysis of genetic variants through aggregation of homologous human protein domains. *Hum Mutat*. 2019;40:1030–8.
23. <https://stuart.radboudumc.nl/metadome/method>.
24. <https://gnomad.broadinstitute.org/>.
25. Fukao T, Mitchell G, Sass JO, Hori T, Orii K, Aoyama Y. Ketone body metabolism and its defects. *J Inher Metab Dis*. 2014;37:541–51.
26. Fisel P, Schaeffeler E, Schwab M. Clinical and functional relevance of the Monocarboxylate Transporter family in disease pathophysiology and drug therapy. *Clin Transl Sci*. 2018;11:352–64.
27. Felmlee MA, Jones RS, Rodriguez-Cruz V, Follman KE, Morris ME. Monocarboxylate transporters (SLC16): function, regulation, and role in health and disease. *Pharmacol Rev*. 2020;72:466–85.
28. Jha MK, Lee Y, Russell KA, Yang F, Dastgheyb RM, Deme P, et al. Monocarboxylate transporter 1 in Schwann cells contributes to maintenance of sensory nerve myelination during aging. *Glia*. 2020;68:161–77.
29. Clarke D. Circulation and energy metabolism of the brain. In: Agranoff BW, Siegel GJ, editors. *Basic neurochemistry molecular, cellular and medical aspects*. 6th ed. Philadelphia: Lippincott-Raven; 1999.
30. Magistretti PJ, Allaman I. A cellular perspective on brain energy metabolism and functional imaging. *Neuron*. 2015;86:883–901.
31. Durnin J. Basal metabolic rate in man 1981. <http://www.fao.org/3/m2845e/m2845e00.htm>. Accessed 22 May 2021.
32. Vannucci RC, Vannucci SJ. Glucose metabolism in the developing brain. *Semin Perinatol*. 2000;24:107–15.
33. Jha MK, Morrison BM. Glia-neuron energy metabolism in health and diseases: new insights into the role of nervous system metabolic transporters. *Exp Neurol*. 2018;309:23–31.
34. Wyss MT, Jolivet R, Buck A, Magistretti PJ, Weber B. In vivo evidence for lactate as a neuronal energy source. *J Neurosci*. 2011;31:7477–85.
35. Sobieski C, Warikoo N, Shu HJ, Mennerick S. Ambient but not local lactate underlies neuronal tolerance to prolonged glucose deprivation. *PLoS ONE*. 2018;13:e0195520.
36. van Hall G, Strømstad M, Rasmussen P, Jans O, Zaar M, Gam C, et al. Blood lactate is an important energy source for the human brain. *J Cereb Blood Flow Metab*. 2009;29:1121–9.
37. Lee Y, Morrison BM, Li Y, Lengacher S, Farah MH, Hoffman PN, et al. Oligodendroglia metabolically supports axons and contribute to neurodegeneration. *Nature*. 2012;487:443–8.
38. Nehlig A, Pereira de Vasconcelos A. Glucose and ketone body utilization by the brain of neonatal rats. *Prog Neurobiol*. 1993;40:163–221.
39. Erecinska M, Cherian S, Silver IA. Energy metabolism in mammalian brain during development. *Prog Neurobiol*. 2004;73:397–445.
40. Dombrowski GJ Jr, Swiatek KR, Chao KL. Lactate, 3-hydroxybutyrate, and glucose as substrates for the early postnatal rat brain. *Neurochem Res*. 1989;14:667–75.
41. Ivanov A, Mukhtarov M, Bregestovski P, Zilberter Y. Lactate effectively covers energy demands during neuronal network activity in neonatal hippocampal slices. *Front Neuroenerg*. 2011;3:2.
42. Hawkins RA, Williamson DH, Krebs HA. Ketone-body utilization by adult and suckling rat brain in vivo. *Biochem J*. 1971;122:13–8.
43. Magistretti PJ, Pellerin L. Cellular mechanisms of brain energy metabolism and their relevance to functional brain imaging. *Philos Trans R Soc Lond B Biol Sci*. 1999;354:1155–63.
44. Morris AA. Cerebral ketone body metabolism. *J Inher Metab Dis*. 2005;28:109–21.
45. Rinholm JE, Hamilton NB, Kessar N, Richardson WD, Bergersen LH, Attwell D. Regulation of oligodendrocyte development and myelination by glucose and lactate. *J Neurosci*. 2011;31:538–48.
46. Sánchez-Abarca LI, Taberero A, Medina JM. Oligodendrocytes use lactate as a source of energy and as a precursor of lipids. *Glia*. 2001;36:321–9.
47. Ichihara Y, Doi T, Ryu Y, Nagao M, Sawada Y, Ogata T. Oligodendrocyte progenitor cells directly utilize lactate for promoting cell cycling and differentiation. *J Cell Physiol*. 2017;232:986–95.
48. Fünfschilling U, Supplie LM, Mahad D, Boretius S, Saab AS, Edgar J, et al. Glycolytic oligodendrocytes maintain myelin and long-term axonal integrity. *Nature*. 2012;485:517–21.
49. Cogliati S, Frezza C, Soriano ME, Varanita T, Quintana-Cabrera R, Corrado M, et al. Mitochondrial cristae shape determines respiratory chain super-complexes assembly and respiratory efficiency. *Cell*. 2013;155:160–71.

## Publisher's Note

Springer Nature remains neutral with regard to jurisdictional claims in published maps and institutional affiliations.

Ready to submit your research? Choose BMC and benefit from:

- fast, convenient online submission
- thorough peer review by experienced researchers in your field
- rapid publication on acceptance
- support for research data, including large and complex data types
- gold Open Access which fosters wider collaboration and increased citations
- maximum visibility for your research: over 100M website views per year

At BMC, research is always in progress.

Learn more [biomedcentral.com/submissions](https://biomedcentral.com/submissions)

